Observations of swash zone velocities: A note on friction coefficients

B. Raubenheimer and Steve Elgar
Woods Hole Oceanographic Institution, Woods Hole, Massachusetts, USA

R. T. Guza
Scripps Institution of Oceanography, La Jolla, California, USA

Received 28 March 2003; revised 6 October 2003; accepted 10 November 2003; published 30 January 2004.

[1] Vertical flow structure and turbulent dissipation in the swash zone are estimated using cross-shore fluid velocities observed on a low-sloped, fine-grained sandy beach [*Raubenheimer*, 2002] with two stacks of three current meters located about 2, 5, and 8 cm above the bed. The observations are consistent with an approximately logarithmic vertical decay of wave orbital velocities within 5 cm of the bed. The associated friction coefficients are similar in both the uprush and downrush, as in previous laboratory results. Turbulent dissipation rates estimated from velocity spectra increase with decreasing water depth from $O(400\ cm^2/s^3)$ in the inner surf zone to $O(1000\ cm^2/s^3)$ in the swash zone. Friction coefficients in the swash interior estimated with the logarithmic model and independently estimated by assuming that turbulent dissipation is balanced by production from vertical shear of the local mean flow and from wave breaking are between 0.02 and 0.06. These values are similar to the range of friction coefficients (0.02–0.05) recently estimated on impermeable, rough, nonerodible laboratory beaches and to the range of friction coefficients (0.01–0.03) previously estimated from field observations of the motion of the shoreward edge of the swash (run-up). *INDEX TERMS:* 4546 Oceanography: Physical: Nearshore processes; 4560 Oceanography: Physical: Surface waves and tides (1255); 4568 Oceanography: Physical: Turbulence, diffusion, and mixing processes; *KEYWORDS:* beach, swash, waves

Citation: Raubenheimer, B., S. Elgar, and R. T. Guza (2004), Observations of swash zone velocities: A note on friction coefficients, *J. Geophys. Res.*, *109*, C01027, doi:10.1029/2003JC001877.

1. Introduction

[2] Bed friction and turbulence are important to wave run-up and sediment transport in the swash zone, the region where the beach is alternately covered and uncovered by waves. Many studies of friction coefficients and turbulent dissipation rates have focused on the surf zone, where breaking wave-induced turbulence dominates wave energy dissipation [e.g., *Thornton and Guza*, 1983]. Surf zone friction coefficients c_f ranging from 0.0007 to 0.0060 have been estimated by fitting model predictions to observed mean alongshore currents [e.g., *Whitford and Thornton*, 1996; *Feddersen et al.*, 1998]. Breaking waves potentially increase c_f by vertically mixing surface-generated turbulence to the seafloor [e.g., *Church and Thornton*, 1993; *Feddersen et al.*, 1998], or potentially decrease c_f by destroying bedforms and by increasing stratification from suspended sediments [*Trowbridge and Elgar*, 2001]. In the outer surf zone, breaking wave turbulence does not reach the seafloor, and the near-bed turbulent dissipation appears to be balanced by shear production [*Trowbridge and Elgar*, 2001]. In contrast, in the middle and inner surf zone, some turbulence reaches the seafloor [e.g., *George et al.*, 1994; *Cox and Kobayashi*, 2000]. Inner surf zone estimates of turbulent dissipation based on velocity spectra and an inertial range model suggest that the dissipation rate is $O(100\ cm^2/s^3)$, and increases toward the shore [*George et al.*, 1994; *Rodriguez et al.*, 1999]. The relevance of the surf zone results to the swash zone is unclear, because the turbulent front faces of uprushing broken waves in the swash zone are sometimes in contact with the bed, and the shallow swash zone water depths may affect the thickness and evolution of the turbulent bottom boundary layer.

[3] Laboratory observations of the vertical structure of cross-shore orbital velocities over impermeable, rough beds in the swash zone show evidence of a logarithmic bottom boundary layer, with $0.02 \leq c_f \leq 0.05$ in both the uprush and downrush [*Cox et al.*, 2001; *Petti and Longo*, 2001; *Archetti and Brocchini*, 2002]. Laboratory measurements of turbulent fluctuations in the swash zone suggest that breaking wave-driven (bore) turbulence dominates during the uprush, while bed-generated turbulence dominates during the downrush [*Petti and Longo*, 2001; *Cowen et al.*, 2003]. Velocity spectra show inertial subranges in which the energy decreases as $f^{-5/3}$, where f is frequency.

[4] There are few field observations of swash zone flows, and thus the applicability of the laboratory observations to

0148-0227/04/2003JC001877$09.00

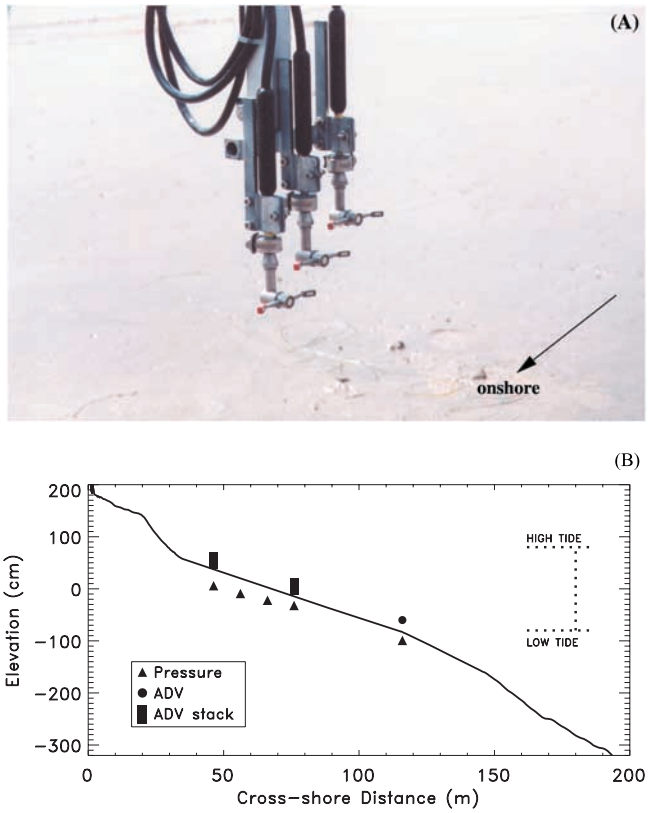

Figure 1. (a) Stack of 3 acoustic Doppler velocimeters (ADV). (b) Elevation of the seafloor relative to mean sea level (curve) versus cross-shore distance x on 28 September 2000. Symbols indicate locations of the two ADV stacks (rectangles), a single downward looking ADV (circle), and buried pressure sensors (triangles). The beach slope was about 0.02 between x = 30 and 120 m. The beach was surveyed about every other day. Daily tide ranges were between about 1 and 2 m.

natural beaches with permeable beds, alongshore flows, and suspended sediments is unknown. Comparisons of the motion of the landward edge of the run-up owing to individual bores on natural beaches with a ballistic model [e.g., *Shen and Meyer*, 1963] suggest that swash edge friction coefficients may be larger in the downrush than in the uprush [*Hughes*, 1995; *Puleo and Holland*, 2001]. Differences between the field estimates of swash edge friction coefficients and the laboratory c_f, which were similar in the uprush and downrush, were attributed to differences between friction at the landward swash edge and in the flow interior, or to a breakdown of the assumptions of ballistic motion at the landward edge (e.g., neglecting infiltration and pressure gradients) and of a logarithmic layer in the flow interior.

[5] Here, the vertical structure of cross-shore fluid velocities observed in the swash zone on a low-sloped beach is shown to be roughly logarithmic, consistent with laboratory results. Corresponding friction coefficients in the swash interior are ≈0.03 in both the uprush and downrush. Similar estimates of c_f (≈0.04) are obtained by balancing turbulent dissipation with production by near-bed fluid shear and by wave breaking. Wave breaking contributes to the total near-bed turbulence in the swash and inner surf zones.

2. Field Experiment and Data Processing

[6] Wave-induced pressure and velocity fluctuations were measured for 16 days during daylight hours in September and October 2000 along a cross-shore transect extending from the shoreline to about 60-cm mean water depth (at mean tide level) on the low-sloped (≈0.02), fine-grained (mean diameter ≈0.02 cm) Scripps Beach near La Jolla, California (Figure 1). The observed cross-shore variation of pressure and velocity has been modeled well with the nonlinear shallow water equations [*Raubenheimer*, 2002]. Here, vertical stacks of sensors (not discussed by *Raubenheimer* [2002]) are used to estimate c_f from the observed vertical flow variations and from the turbulent energy balance in the swash zone.

[7] Velocities and pressures were acquired at 16 Hz for 3072 s (51.2 min) starting every hour. To measure cross-shore fluid velocities, two sets of 3 vertically stacked two-dimensional acoustic Doppler velocimeters (ADV) (Figure 1a) were oriented so that the transducers faced alongshore (north) within 2°. The cylindrical sample volume of each sensor is centered about 5 cm (alongshore) from the center transducer, and has a horizontal length (in the alongshore direction) of about 0.72 cm and vertical radius of approximately 0.30 cm. Measured vertical tilts were less than 1°. Elevations z above the sand of the stacked ADVs were measured with reference rods approximately hourly during daylight. At low tide, the stacked sensors were adjusted vertically to maintain constant elevations above the bed. However, owing to sand level changes during tidal cycles, z of the sensors fluctuated, and data were restricted to runs with elevations above the bed of the lowest sensor z_l between about 0.5 and 9.0 cm. During daylight, observers attempted to remove kelp and other floating debris from the swash zone. Data from fouled sensors were discarded. Roughly 50% of the daylight data were considered valid.

[8] Stacked ADVs were separated by 3 cm in the vertical and by 5 cm in the horizontal (cross-shore) direction. Wavelengths of the most energetic waves in the swash zone are much longer than the cross-shore separation of the sensors, and the horizontal separation of the stacked sensors is neglected. Noise in the velocity signal can be owing to sampling errors, doppler noise, and velocity shear within the sample volume. However, previous studies have shown that ADVs accurately measure mean currents and wave orbital velocities at elevations above the bed equal to or greater than the vertical height of the sample volume (0.30 cm for the current meters used here) [*Voulgaris and Trowbridge*, 1998; *Williams et al.*, 2003]. Furthermore, the noise estimated from the high-frequency tail of the spectrum has been shown to agree well with the theoretically expected noise [*Voulgaris and Trowbridge*, 1998], suggesting that turbulence spectra can be estimated accurately by subtracting noise estimated from the tail of the signal spectrum.

[9] At low tide and between swashes, sensors sometimes were not submerged. Velocities were set to 0.0 cm/s when the strength of the backscattered acoustic signal along any beam indicated the sensor was out of the water. Estimates of water levels using colocated pressure sensors were consis-

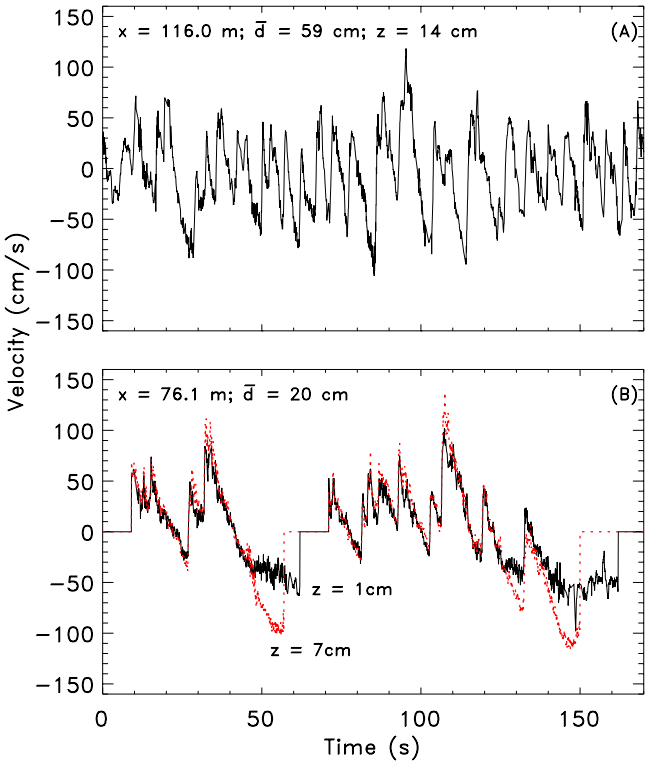

Figure 2. Observed cross-shore velocity (positive onshore) versus time on 10 October (a) in the surf zone at z = 14 cm above the bed in mean water depth $\overline{d}$ = 59 cm and (b) in the swash zone at z = 7 (red dotted curve) and 1 cm (black solid curve) in $\overline{d}$ = 20 cm. For the section of data shown, significant wave heights were 35 and 25 cm for $\overline{d}$ = 59 and 20 cm, respectively.

tent with periods of ADV submergence determined using the acoustic signal strength. Swash runs, defined as runs during which the beach at the instrumented location was uncovered by water for at least 16 consecutive data points (1 s) out of each 8.5 min, correspond to mean depths less than about 25 cm. (Mean water depths are based on time periods when the bed is submerged.) From the 197 hours of valid data collected with the two sensor stacks, roughly 70 hours (including periods between waves when the sensors were not submerged) of swash zone velocities were available. In 25- and 5-cm mean water depths the velocimeters were submerged 98 ± 2% and 25 ± 9% of the time, respectively.

[10] For the near-bed flows considered here, the ADV acoustic pulses may be scattered by suspended sand. However, the 2-ms sediment response time to fluid motions [*Snyder and Lumley*, 1971] is much shorter than the periods of waves and turbulence discussed below, so it is assumed that suspended sediment motions are good indicators of the true horizontal flow [*Zedel and Hay*, 1999]. Excessive scatterers (e.g., bubbles) near the ADV sample volume can reflect sidelobe energy, resulting in noisy velocity estimates. Potentially noisy velocity measurements were identified using the correlations reported by the ADV along each beam [*Elgar et al.*, 2001]. The noise is unbiased, and averaging consecutive samples is expected to provide a good estimate of the flow at low frequencies. In the analysis of flow structure at wave frequencies, velocities with low correlations were replaced with a 1-s running mean of the data when the sensors were submerged [*Elgar et al.*, 2001]. Velocities with low correlations were excluded from the analysis of turbulent dissipation. In most of the data runs used here, less than 3% of the observed velocities had low correlations.

[11] Seaward of the surf zone in 300-cm water depth, the significant wave height H_s (defined as four times the standard deviation of the sea surface elevation fluctuations) ranged from 55 to 104 cm, and the spectral peak frequencies ranged from 0.07 to 0.16 Hz. In the swash and inner surf zones, root mean square wave orbital velocities (σ) were between 28 and 61 cm/s, and the mean flow speed (V, averaged over 51.2-min data runs) ranged from 3 to 19 cm/s. Usually, V was approximately cross-shore directed, waves were nearly normally incident, and the angle (θ) between wave orbital velocities and the mean flow was less than 1.5°.

3. Results

[12] The maximum seaward and shoreward directed cross-shore velocities u observed over several minutes at elevations more than a few cm above the bed were similar in the surf and swash zones (Figure 2; the velocity range is about $-100 \leq u \leq 120$ cm/s in both 59- and 20-cm water depth, and see *Raubenheimer* [2002]). However, within about 5 cm of the bed, u decreased with decreasing z, with larger differences in flow magnitude for longer period waves (e.g., time = 50 and 150 s in Figure 2b). Note that as the water depth thinned during the rundown, the lower sensor was submerged longer than the upper sensor. In the analyses below, the velocities at all three elevations were excluded when the upper sensor was out of the water (e.g., root mean square (rms) fluctuations were calculated using only measurements when all three sensors were submerged.)

[13] The vertical structure of the observed cross-shore velocities was fit to a logarithmic model

$$u = \frac{u_*}{\kappa} \ln \frac{z - d_*}{z_0}, \tag{1}$$

where u_* is the shear velocity, κ is the Von Kármán constant (approximated as 0.4), d_* is the displacement distance, and z_0 is the bottom roughness. Orbital velocities (u_h and u_l) observed at the highest and lowest sensors (located at elevations z_h and z_l above the bed) are related by

$$u_l = u_h \left(\ln \frac{z_l - d_*}{z_0} \right) \Big/ \left(\ln \frac{z_h - d_*}{z_0} \right). \tag{2}$$

Following *Jackson* [1981] and *Cox et al.* [1996], d_* was estimated as $0.7 d_{50}$, where d_{50} is the median grain size (≈0.02 cm). The average (± standard deviation) bottom roughness z_0 = 0.061 (±0.015) was estimated following *Nielsen* [1992, equations (2.2.5) and (3.6.10)]. The sensor elevations, which changed by as much as 4 cm between hourly measurements, were assumed to vary linearly in time over each 51.2-min data run. Using the acoustic signal strength to estimate times of burial and unburial of sensors,

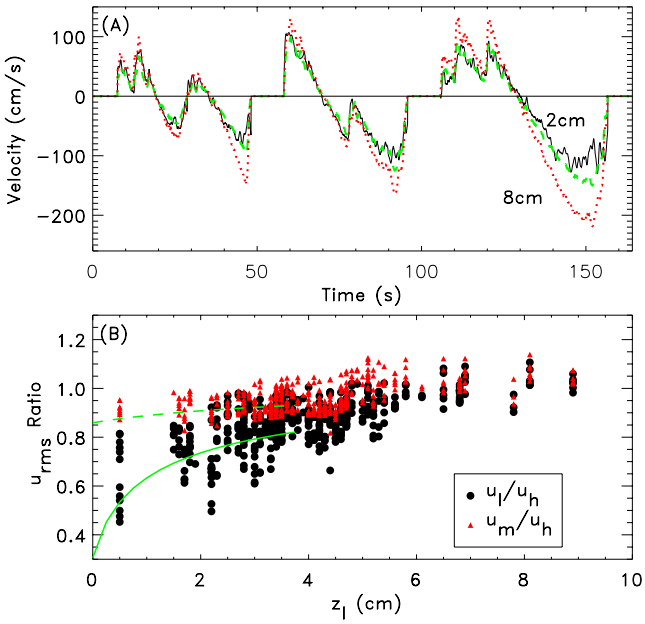

Figure 3. (a) Observed band-passed ($0.004 \leq f \leq 2.0$ Hz) cross-shore velocities on 11 October at 2 (solid black curve) and 8 cm (dotted red curve) above the bed and velocities predicted 2 cm above the bed (dashed green curve) assuming a logarithmic vertical structure (equation (2)) versus time. (b) Observed (symbols) and predicted (green curves; equation (2) with $z_0 = 0.06$) ratios of root mean square orbital swash velocities (u_{rms} ratios) at the lower and upper sensors (black circles and green solid curve, u_l/u_h), and at the middle and upper sensors (red triangles and green dashed curve, u_m/u_h) versus elevation of the lowest sensor z_l.

it is estimated that sensor elevations may have deviated 1 to 2 cm from this linear variation.

[14] Observed band-passed ($0.004 \leq f \leq 2.0$ Hz) velocity time series at the lowest sensor (Figure 3a) were roughly consistent with a logarithmic profile (equation (2)) during both the uprush and downrush, similar to laboratory observations on rough beds [*Cox et al.*, 2001; *Petti and Longo*, 2001; *Archetti and Brocchini*, 2002]. The ratios of root mean square swash zone velocity fluctuations (i.e., velocity attenuation) measured at the lower and upper sensors (black circles in Figure 3b) and at the middle and upper sensors (red triangles in Figure 3b), and the increase of attenuation with decreasing z_l, were predicted qualitatively for 493 8.5-min sections of data. Root mean square errors (i.e., differences between observed and theoretical ratios) were 0.11 and 0.05 for u_l/u_h and u_m/u_h, respectively. Deviations between the observed and theoretical ratios can result from errors ($\approx$1 to 2 cm) in the estimated z_l. If the observed z_l are adjusted by up to 1 cm to improve the agreement with the theory, the rms errors are about half as large (0.06 and 0.03 for u_l/u_h and u_m/u_h, respectively). In contrast, 1 cm errors in z_l of the opposite sign would increase the errors. The results are not sensitive to factor 5 changes in d_*, but errors in estimating z_0 may affect the modeled velocity attenuation at the lowest z_l. For the data presented here and in *Raubenheimer* [2002] with $0.5 \leq z_l \leq 5.0$ cm, 80% of the observed rms ratios u_l/u_h were greater than 0.8.

[15] The logarithmic model (equations (1) and (2)) is expected to apply when $z/\overline{d} \ll 1$ (where $\overline{d}$ is the mean water depth) and $z/\delta \ll 1$ (where δ is the thickness of the wave boundary layer). For the data with $0.5 \leq z_l \leq 4.0$ cm, $0.04 \leq z/\overline{d} \leq 0.58$ and $0.002 \leq z/\delta \leq 1.0$, where δ was estimated as $u_* T/2$, with T the wave period corresponding to the centroidal frequency of the observed velocity fluctuations. Although the assumptions used to derive equation (2) sometimes were violated, the agreement between the predicted and observed attenuation (Figure 3b) did not degrade as z_l increased. Although the many sources of error preclude quantitative confirmation of a logarithmic boundary layer, the results are qualitatively consistent with laboratory results [*Cox et al.*, 2001; *Archetti and Brocchini*, 2002].

[16] For three 51.2-min inner surf and swash runs with approximately constant sensor elevation (initial and final elevations differed by less than 0.4 cm) and with run-averaged $z_l \leq 2.5$ cm, infragravity, swell, and sea ($0.01 \leq f \leq 0.20$ Hz) velocity fluctuations decreased toward the bed,

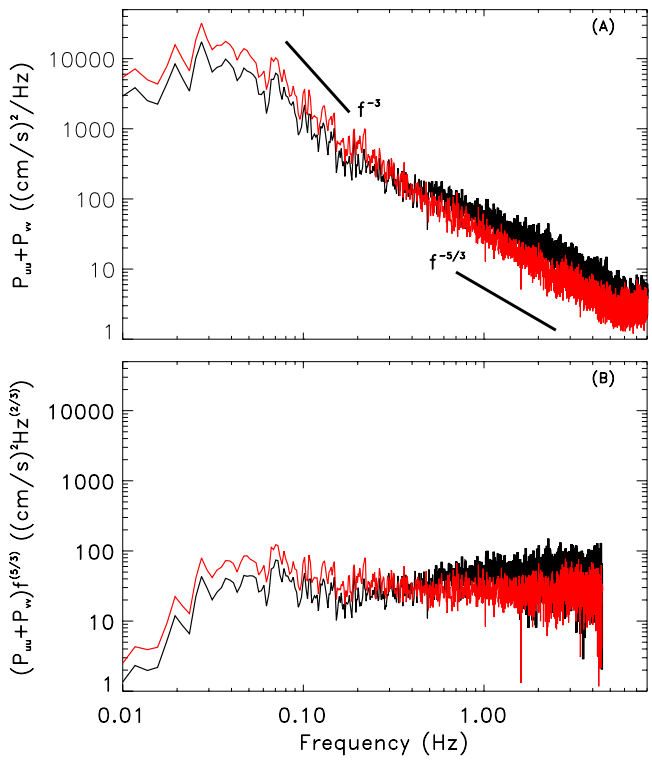

Figure 4. (a) Sum of cross-shore (P_{uu}) and alongshore (P_{vv}) velocity spectral density and (b) modified velocity spectral density ($(P_{uu} + P_{vv} - noise)f^{5/3}$) versus frequency. Measurements were 7.5 (red curves) and 1.5 cm (black curves) above the bed in the swash zone (mean water depth about 15 cm) on 3 October. The modified velocity spectrum is expected to be constant in the inertial subrange. The modified spectrum is not shown for $f > 4.5$ Hz, where the spectral levels approach the noise floor. Velocity spectra are calculated using 51.2-min runs to ensure accurate spectral levels even when the bed is intermittently covered. Spectra were estimated by averaging Fourier transforms of tapered autocovariances from six 8.5-min 16-Hz (unfiltered) time series. Data pairs were excluded from the autocovariances if one or both values were 0.0 cm/s or had a low correlation.

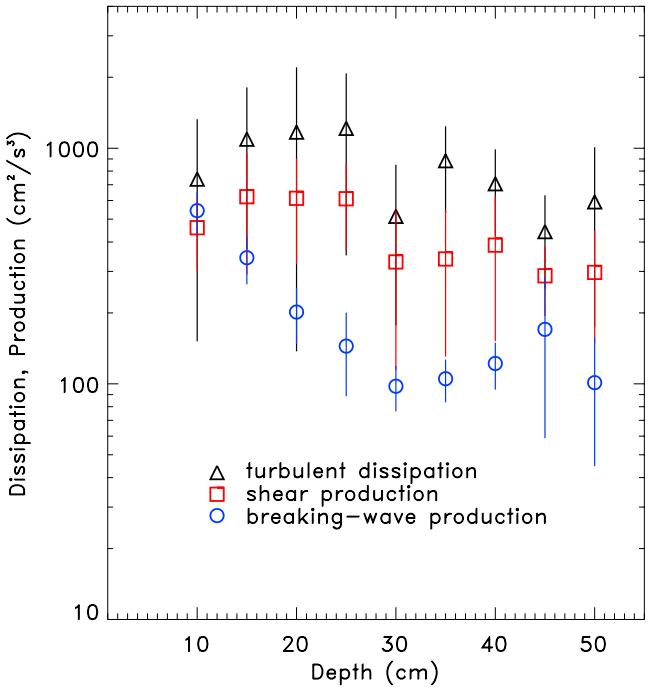

Figure 5. Mean (symbols) and standard deviations (vertical lines) of the turbulent dissipation rate ε (black triangles) estimated from velocity spectra (equation (4)) and magnitude of turbulence production by wave breaking ($-\frac{1}{\rho_0 \overline{d}}\frac{\partial F_x}{\partial x}$) (blue circles) and by near-bed fluid shear ($c_f\overline{(u^2+v^2)^{1/2}u}\frac{\partial \overline{u}}{\partial z}$) (red squares) estimated from equation (6) with $c_f = 0.04$ versus mean water depth $\overline{d}$. Data bins are $\overline{d} \pm 2.5$ cm. The correlation r between mean binned values of ϵ and $\overline{d}$ is -0.66. For unbinned data, ϵ was correlated with production by shear ($r = 0.74$). To estimate total dissipation (and turbulence production), the terms would need to be integrated over time and the water column. For example, total energy losses (per unit volume) over a 51.2-min run are proportional to the percent of time the sensor is submerged, ranging from about 100% for $\overline{d} > 25$ cm to about 25% for $\overline{d} = 5$ cm.

while high-frequency fluctuations ($0.5 \le f \le 6.0$ Hz) increased toward the bed (Figure 4a), consistent with bed-generated turbulence in a near-bed constant stress region with a logarithmic orbital velocity profile. In contrast to the results shown in Figure 4, but consistent with previous inner surf zone observations for $z \ge 10$ cm [*Rodriguez et al.*, 1999], high-frequency energy increased with increasing z for swash and inner surf runs with $z_l > 4.0$ cm (not shown), possibly owing to downward mixing of surface-generated, breaking wave turbulence. Similar to previous observations in the surf zone [e.g., *Thornton*, 1979; *George et al.*, 1994; *Trowbridge and Elgar*, 2001], the velocity energy levels in all runs decreased approximately as f^{-3} between the spectral peak frequency and about 0.20 Hz, consistent with saturated waves or an inverse energy cascade, and as $f^{-5/3}$ for $1.5 < f < 4.5$ Hz, consistent with an inertial subrange. Unlike laboratory studies [*Cowen et al.*, 2003], only a single inertial subrange was observed.

[17] Friction coefficients for 382 8.5-min swash zone data runs with $1.0 \le z_l \le 4.0$ cm (where the logarithmic model is approximately valid) were estimated using the quadratic drag law as

$$c_f = 2(\overline{u_*|u_*|}) \Big/ (\overline{u_h|u_h|}), \tag{3}$$

where the overbar () represents a time average over all nonzero velocity data in each record. Band-passed velocities observed at the lowest sensor were used to estimate u_* from equation (1), and velocities observed at the upper sensor (u_h) were assumed to represent outer flow conditions. Friction coefficients for the uprush and downrush were not statistically different, with average values of $c_f = 0.03 \pm 0.01$, consistent with laboratory studies [*Cox et al.*, 2001; *Archetti and Brocchini*, 2002].

[18] Alternatively, friction coefficients can be calculated from turbulent dissipation rates estimated from cross-shore and alongshore ($P_{uu}(f) + P_{vv}(f)$) velocity spectra and an inertial range turbulence model. Dissipation rates ϵ were estimated from the velocity spectra in the $f^{-5/3}$ region for 51.2-min swash and inner surf zone runs [*Trowbridge and Elgar*, 2001],

$$\epsilon = \left[\frac{55}{21}(P_{uu}(f) + P_{vv}(f) - noise) \cdot (2\pi f)^{5/3} V^{-2/3}\alpha^{-1} I\left(\frac{\sigma}{V}, \theta\right)^{-1}\right]^{3/2}, \tag{4}$$

where α is the empirical Kolmogorov constant (estimated as 1.5 following *Grant et al.* [1962]), and

$$I\left(\frac{\sigma}{V}, \theta\right) = \frac{1}{\sqrt{2\pi}}\left(\frac{\sigma}{V}\right)^{2/3}\int_{-\infty}^{\infty}\left[x^2 - 2\frac{V}{\sigma}\cos(\theta)x + \frac{V^2}{\sigma^2}\right]^{1/3} \cdot \exp\left(-\frac{1}{2}x^2\right)dx. \tag{5}$$

The Kolmogorov inertial subrange model requires that $kz \gg 1$, where the eddy wave number k is approximated as $2\pi f/u_{rms}$, to ensure that eddies are small relative to the distance to the bed. Furthermore, the water depth ideally should be much larger than the eddies to avoid constraints on the turbulence scales by proximity to the water surface. However, the Kolmogorov model is reasonably accurate for velocity fluctuations parallel to the dominant flow when $2\pi fz/u_{rms} > 1$ [*Kaimal et al.*, 1972], and for $z/\overline{d} \le 0.5$ [*Nezu and Nakagawa*, 1993]. Here, data were restricted to 81 runs with $\overline{d} \le 50$ cm, $1.5 \le z \le 7.0$ cm, $1.1 < 2\pi fz/u_{rms} \le 7.6$ at 1.5 Hz, and $0.03 < z/\overline{d} < 0.49$.

[19] Noise energy levels were estimated as the average spectral level in the frequency range $6.0 \le f \le 7.0$ Hz. Modified spectral levels ($((P_{uu}(f) + P_{vv}(f) - noise)f^{5/3}$; e.g., Figure 4b) were averaged over frequencies (typically $1.5 \le f \le 4.5$ Hz) for which the mean levels over 0.2 Hz wide frequency bands were constant to within ±25%. The frozen turbulence assumption (i.e., that the velocities advecting turbulence are steady over the record length) used in the derivation of equation (4) was not satisfied. However, *George et al.* [1994] found that dissipation estimates from spectra of 8.5-min records were within a factor of 2 of estimates from spectra of 0.125-s records in

which the turbulence-advecting velocities were nearly constant. Similar to previous observations across the surf zone [*George et al.*, 1994; *Rodriguez et al.*, 1999], estimated dissipation rates increased with decreasing water depth across the inner surf zone (Figure 5). In about 45-cm water depth, $\epsilon \approx 400$ cm^{2}s^{-3}, consistent with *Flick and George* [1990].

[20] Friction coefficients were estimated assuming turbulent dissipation is balanced by the sum of turbulent energy production by near-bed fluid shear and by wave breaking,

$$\epsilon = c_f \overline{(u^2 + v^2)^{1/2} u} \frac{\partial \overline{u}}{\partial z} - \frac{1}{\rho_0 \overline{d}} \frac{\partial F_x}{\partial x}, \quad (6)$$

where the bottom stress is approximated by a quadratic drag law, $\overline{u}$ is the mean cross-shore current (based on periods when the sensor was submerged), v is the alongshore flow, and ρ_0 is the (constant) fluid density. The breaking wave dissipation $\partial f_x/\partial x$ is assumed to be distributed evenly across the water column. Using linear theory to calculate wave energy E, and assuming shoreward progressive, normally incident shallow water waves, the cross-shore (x) component of the wave-induced energy flux (F_x) owing to swell and sea ($0.05 \leq f \leq 0.20$ Hz) is

$$F_x = E c_g = \frac{\rho_0 g^{3/2}}{16} H_s^2 \overline{d}^{1/2}, \quad (7)$$

where c_g is the linear group velocity, and g is gravitational acceleration. Substitution of equation (7) into equation (6) yields

$$c_f = \left[\epsilon + \frac{g^{3/2}}{16\overline{d}} \frac{\partial}{\partial x}\left(H_s^2 \overline{d}^{1/2}\right)\right] \left[\overline{(u^2 + v^2)^{1/2} u} \frac{\partial \overline{u}}{\partial z}\right]^{-1}. \quad (8)$$

The cross-shore gradients of H_s and $\overline{d}$ were evaluated using observations (averaged over the times for which the velocimeter used to estimate ε was submerged) from pairs of pressure sensors located at x = 76.0 and 66.2 m, and at x = 56.2 and 46.3 m (Figure 1a). For these data, breaking induced turbulence accounted for approximately 26% ± 15% of the total near-bed turbulent dissipation in the swash and inner surf zone (Figure 5). Although the rate of breaking induced production increases shoreward, the water depth and the percent of time the beach is submerged decrease shoreward, and thus the total breaking induced production (integrated over the water column and time) may decrease shoreward across the swash zone following bore collapse. Limiting the data to 49 swash zone runs with $1.5 \leq z_l \leq 4.0$, similar to the elevation range used in the logarithmic analysis, the estimated swash zone c_f is 0.04 ± 0.02.

4. Discussion

4.1. Errors in Friction Coefficient Estimates

[21] Errors in the c_f estimated using the logarithmic model (equation (3)) may result from errors in measuring z_l, especially when velocities were observed within 2 cm of the bed. For example, if the true and measured z_l were 2.0 and 1.0 cm, respectively, the friction coefficient would be overpredicted by about 45%. If the true and measured z_l were 1.0 and 2.0 cm, the friction coefficient would be underestimated by about 40%. If the true and measured z_l were 5.0 and 4.0 cm, respectively, the friction coefficient would be overpredicted by about 10%. Alternatively, deviations from a logarithmic structure could result in errors in the estimated friction coefficients. For example, cycling of water through the sand bed (e.g., infiltration and exfiltration) may have little affect on swash velocities and run-up excursions [e.g., *Raubenheimer*, 2002], but may cause stretching or thinning of the bottom boundary layer [*Turner and Masselink*, 1998], resulting in underestimation or overestimation of c_f. Mixing from breaking wave-induced turbulence and stratification caused by bubbles and suspended sediments may cause deviations from a logarithmic layer that could result in overestimation of c_f. In addition, if z_h were less than the boundary layer thickness, and thus u_h were smaller than the outer flow velocities, c_f would be overestimated.

[22] Errors in swash zone c_f estimated from turbulent dissipation (equation (8)) may result from using linear theory to calculate F_x (equation (7)). Estimates of E using the linear theory approximation of equipartition of potential and kinetic energy (as in equation (7)),

$$E = \frac{1}{16} \rho_0 g H_s^2 \quad (9)$$

were lower (by as much as 50%, with the largest differences in about 30-cm water depth) than estimates using

$$E = \frac{\rho_0}{2}\left(\overline{\int_0^{\eta} (u^2 + v^2) dz} + \overline{g\tilde{\eta}^2}\right), \quad (10)$$

where z equals 0 at the seafloor, η is the instantaneous sea surface elevation, and $\tilde{\eta}$ is the deviation of the sea surface relative to the mean water level [see also *Raubenheimer*, 2002]. Owing to the large horizontal separation between the vertical ADV stacks, it was not possible to use equation (10) to estimate the energy gradients in equation (6). Deviations from the linear group velocity ($c_g = (g\overline{d})^{1/2}$) also may cause errors in F_x, and hence in c_f [e.g., *Puleo et al.*, 2003]. Furthermore, wave energy and noise at inertial subrange frequencies (resulting in overprediction of dissipation), constraints on eddy sizes owing to proximity to the bed or water surface, turbulent fluctuations at frequencies used to estimate noise (resulting in underprediction of dissipation), and violations of the assumptions of frozen turbulence over 8.5-min records [e.g., *George et al.*, 1994] may cause errors in estimates of c_f.

4.2. Comparison With Previous Field Estimates

[23] Field measurements of run-up fluctuations [*Raubenheimer et al.*, 1995] and swash zone velocities [*Raubenheimer*, 2002] have been predicted reasonably well with a model based on the nonlinear shallow water equations (NSWE) using a constant friction coefficient $c_f = 0.015$, determined by fitting model predictions to both swash and surf zone observations. Alternatively, by fitting observations of the observed motion of the landward edge of the run-up to a ballistic model based on a special case of the nonlinear shallow water equations [e.g., *Shen and*

Meyer, 1963], swash edge friction coefficients were estimated to be up to a factor 10 larger in the downrush than the uprush [*Puleo and Holland*, 2001]. However, after accounting for neglected terms including cross-shore pressure gradients and the effects of beach permeability, swash edge coefficients were estimated to be roughly 0.01 in the uprush and 0.01 to 0.03 in the downrush [*Puleo and Holland*, 2001]. Downrush edge coefficients may decrease with decreasing exfiltration [*Puleo and Holland*, 2001], and thus uprush and downrush edge coefficients may be similar (0.01) to each other on the fine-grained, low-permeability Scripps Beach. These results are not inconsistent with the uprush edge friction coefficients ($\approx$0.025 when corrected for a factor 4 difference in the constant used to relate friction and bed stress) estimated by *Hughes* [1995] on a steep, permeable beach. The swash edge coefficients (0.01–0.03) are smaller than the swash interior c_f presented here, possibly because swash edge estimates based on Lagrangian measurements of the motion of the water edge are inherently different than swash interior c_f based on Eulerian observations of the fluid velocities, as suggested by *Puleo and Holland* [2001]. Despite the many potential sources of discrepancies between different methods, c_f estimated here with the logarithmic- and dissipation-based methods (0.03 $\pm$ 0.01 and 0.04 $\pm$ 0.02, respectively) is similar to the previous laboratory logarithmic-based (0.02 to 0.05) and field swash-edge coefficients (0.01 to 0.03).

5. Conclusions

[24] The vertical structure of cross-shore orbital velocities observed in the swash zone of a low-sloped, fine-grained beach is approximately logarithmic within 5 cm of the bed. Turbulent dissipation rates are consistent with previous estimates ($O(400\ \mathrm{cm^2 s^{-3}})$) in the inner surf zone, and increase with decreasing water depth to $O(1000\ \mathrm{cm^2 s^{-3}})$ in the swash zone. Swash zone bed friction coefficients c_f estimated assuming a logarithmic flow structure ($c_f = 0.03 \pm 0.01$) are similar to values based on dissipation rates ($c_f = 0.04 \pm 0.02$), and to previous estimates. Logarithmic-based c_f estimates are similar during the uprush and downrush, as in prior laboratory studies. A crude balance between turbulent dissipation and turbulent production by near-bed fluid shear and wave breaking suggests that wave breaking is important to near-bed turbulence in the swash and inner surf zones.

Appendix A

[25] An inner surf zone run in which the sensors were always submerged and the correlations remained high was used to determine the effect on high-frequency spectral levels of excluding data pairs from the autocovariance calculations. Spectral estimates with (1) no velocity data excluded ($\overline{d}$ = 38 cm), and with data excluded when the instantaneous water depth was less than (2) 23 cm (5% data excluded), (3) 28 cm (16% data excluded), and (4) 38 cm (50% data excluded) were compared with each other. In these test cases, the rate of decrease of high-frequency spectral levels with increasing frequency was not affected significantly by the exclusion of data pairs, and the magnitude of the high-frequency spectral levels for cases 2–4 relative to those for the raw data (case 1) increased by less than 25%. The smallest relative change in high-frequency spectral level magnitudes (1%) occurred for case 4.

[26] **Acknowledgments.** This research was supported by ONR and NSF. Engineering and field support were provided by William Boyd, Dennis Darnell, Kimball Millikan, Anil Shukla, Kent Smith, Brian Woodward, and Lynn Yarmey. John Trowbridge is thanked for providing assistance and advice with the data analysis. The anonymous reviewers provided helpful comments and suggestions.

References

Archetti, R., and M. Brocchini (2002), An integral swash zone model with friction: An experimental and numerical investigation, *Coastal Eng.*, *45*, 89–110.

Church, J. C., and E. B. Thornton (1993), Effects of breaking wave induced turbulence within a longshore current model, *Coastal Eng.*, *20*, 1–28.

Cowen, E. A., I. M. Sou, P. L.-F. Liu, and B. Raubenheimer (2003), PIV measurements within a laboratory generated swash zone, *J. Eng. Mech.*, *129*, 1119–1129.

Cox, D. T., and N. Kobayashi (2000), Identification of intense, intermittent coherent motions under shoaling and breaking waves, *J. Geophys. Res.*, *105*, 14,223–14,236.

Cox, D. T., N. Kobayashi, and A. Okayasu (1996), Bottom shear stress in the surf zone, *J. Geophys. Res.*, *101*, 14,337–14,348.

Cox, D. T., W. A. Hobensack, and A. Sukumaran (2001), Bottom stress in the inner surf and swash zone, in *Coastal Engineering: Proceedings of the 27th International Conference on Coastal Engineering held in Sydney, Australia, July 16–21, 2000*, edited by B. L. Edge, Am. Soc. of Civ. Eng., Reston, Va.

Elgar, S., B. Raubenheimer, and R. T. Guza (2001), Current meter performance in the surf zone, *J. Atmos. Oceanic Technol.*, *18*, 1735–1746.

Feddersen, F., R. T. Guza, S. Elgar, and T. H. C. Herbers (1998), Alongshore momentum balances in the nearshore, *J. Geophys. Res.*, *103*, 15,667–15,676.

Flick, R., and R. George (1990), Turbulence scales in the surf and swash, in *Coastal Engineering:Proceedings of the International Conference held July 2–6, 1990 in Delft, the Netherlands*, edited by B. L. Edge, pp. 557–569, Am. Soc. of Civ. Eng., Reston, Va.

George, R., R. Flick, and R. T. Guza (1994), Observations of turbulence in the surf zone, *J. Geophys. Res.*, *99*, 801–810.

Grant, H. L., R. W. Stewart, and A. Moilliet (1962), Turbulence spectra from a tidal channel, *J. Fluid Mech.*, *12*, 241–263.

Hughes, M. G. (1995), Friction factors for wave uprush, *J. Coastal Res.*, *11*, 1089–1098.

Jackson, P. S. (1981), On the displacement height in the logarithmic velocity profile, *J. Fluid Mech.*, *111*, 15–25.

Kaimal, J. C., I. Izumi, and O. R. Cote (1972), Spectral characteristics of surface layer turbulence, *Q. J. R. Meteorol. Soc.*, *98*, 563–589.

Nezu, I., and H. Nakagawa (1993), *Turbulence in Open-channel Flows*, 281 pp., A. A. Balkema, Brookfield, Vt.

Nielsen, P. (1992), *Coastal Bottom Boundary Layers and Sediment Transport*, 324 pp., World Sci., River Edge, N. J.

Petti, M., and S. Longo (2001), Turbulence experiments in the swash zone, *Coastal Eng.*, *43*, 1–24.

Puleo, J. A., and K. T. Holland (2001), Estimating swash zone friction coefficients on a sandy beach, *Coastal Eng.*, *43*, 25–40.

Puleo, J. A., G. Farquharson, S. J. Frasier, and K. T. Holland (2003), Comparison of optical and radar measurements of surf and swash zone velocity fields, *J. Geophys. Res.*, *108*(C5), 3100, doi:10.1029/2002JC001483.

Raubenheimer, B. (2002), Observations and predictions of fluid velocities in the surf and swash zones, *J. Geophys. Res.*, *107*, 3190, doi:10.1029/2001JC001264.

Raubenheimer, B., R. T. Guza, S. Elgar, and N. Kobayashi (1995), Swash on a gently sloping beach, *J. Geophys. Res.*, *100*, 8751–8760.

Rodriguez, A., A. Sanchez-Arcilla, J. M. Redondo, and C. Mösso (1999), Macroturbulence measurements with electromagnetic and ultrasonic sensors: A comparison under high-turbulent flows, *Exp. Fluids*, *27*, 31–42.

Shen, M. C., and R. E. Meyer (1963), Climb of a bore on a beach, 3, runup, *J. Fluid Mech.*, *16*, 113–125.

Snyder, W. H., and J. L. Lumley (1971), Some measurements of particle velocity autocorrelation functions in a turbulent flow, *J. Fluid Mech.*, *48*, 41–71.

Thornton, E. B. (1979), Energetics of breaking waves within the surf zone, *J. Geophys. Res.*, *84*, 4931–4938.

Thornton, E. B., and R. T. Guza (1983), Transformation of wave height distribution, *J. Geophys. Res.*, *88*, 5925–5938.

Trowbridge, J. H., and S. Elgar (2001), Turbulence measurements in the surf zone, *J. Phys. Oceanogr.*, *31*, 2403–2417.

Turner, I. L., and G. Masselink (1998), Swash infiltration-exfiltration and sediment transport, *J. Geophys. Res.*, *103*, 30,813–30,824.

Voulgaris, G., and J. H. Trowbridge (1998), Evaluation of the acoustic Doppler velocimeter (ADV) for turbulence measurements, *J. Atmos. Oceanic Technol.*, *15*, 272–289.

Whitford, D. J., and E. B. Thornton (1996), Bed shear stress coefficients for longshore currents over a barred profile, *Coastal Eng.*, *27*, 243–262.

Williams, J. J., P. S. Paul, and P. D. Thorne (2003), Field measurements of flow fields and sediment transport above mobile bed forms, *J. Geophys.*, *108*, 3109, doi:10.1029/2002JC001336.

Zedel, L., and A. E. Hay (1999), A coherent doppler profiler for high-resolution particle velocimetry in the ocean: Laboratory measurements of turbulence and particle flux, *J. Atmos. Oceanic Technol.*, *16*, 1102–1117.

S. Elgar and B. Raubenheimer, Woods Hole Oceanographic Institution, Woods Hole, MA 02543, USA. (britt@whoi.edu)

R. T. Guza, Scripps Institution of Oceanography, La Jolla, CA 92093-0209, USA.